Endotaxial growth mechanisms of Sn Quantum Dots in Si matrix

P. Möck[1], Y. Lei[2], T. Topuria[2], N.D. Browning[3,2], R. Ragan[4*], K.S. Min[4**], and H.A. Atwater[4]

[1] Department of Physics, Portland State University, P.O. Box 751, Portland, OR 97207-0751, pmoeck@pdx.edu
[2] Department of Physics, University of Illinois at Chicago, 845 W. Taylor Street, Chicago, IL 60607-7059
[3] Department of Chemical Engineering and Materials Science, University of California at Davis, One Shields Avenue, Davis, CA 95616; and National Center for Electron Microscopy, MS 72-150, Lawrence Berkeley National Laboratory, Berkeley, CA 94720
[4] Thomas J. Watson Laboratory of Applied Physics, California Institute of Technology, MS 128-95, Pasadena, CA 91125 * now at: Hewlett-Packard Laboratories M/S 1123, 1501 Page Mill Rd., Palo Alto, CA 94304, ** now at: Intel Corporation, California Technology and Manufacturing, MS RNB-2-35, 2200 Mission College Blvd., Santa Clara, CA 95052-8119

ABSTRACT

Two distinct mechanisms for the endotaxial growth of quantum dots in the Sn/Si system were observed by means of analytical transmission electron microcopy. Both mechanisms operate simultaneously during temperature and growth rate modulated molecular beam epitaxy combined with ex situ thermal treatments. One of the mechanisms involves the creation of voids in Si, which are subsequently filled by Sn, resulting in quantum dots that consist of pure α-Sn. The other mechanism involves phase separation and leads to substitutional solid solution quantum dots with a higher Sn content than the predecessor quantum well structures possess. In both cases, the resultant quantum dots possess the diamond structure and the shape of a tetrakaidecahedron. (Sn,Si) precipitates that are several times larger than the typical (Sn,Si) quantum dot possess an essentially octahedral shape.

INTRODUCTION

Self-assembled semiconductor quantum dots (QDs) are expected to lead to *"paradigm changes in semiconductor physics"* [1]. For semiconductor opto-electronic devices, the QD size must be of the order of magnitude of the exciton Bohr radius. The energy band gap of the QDs must be smaller than that of the surrounding semiconductor matrix. No structural defects such as dislocations, which lead to non-radiative recombination, are allowed to exist in the QDs [2].

As α-Sn is a direct, 0.08 eV, band gap semiconductor and substitutional Sn_xSi_{1-x} solution are predicted to possess direct band gaps for $0.9 < x < 1$ [3], QDs in a Si matrix consisting of pure α-Sn or substitutional (Sn,Si) solutions with a sufficiently high Sn content have potential applications as direct band-gap material for cheap and effective optoelectronic and thermo-photovoltaic devices. There are, however, at room temperature a 41.8 % bulk unit cell volume mismatch between α-Sn and Si and an equilibrium solid solubility of Sn in Si of only 0.12 %. This restricts the growth of pseudomorph Sn_xSi_{1-x} layers on Si by molecular beam epitaxy (MBE) [4-7] to a Sn content of about 10 % and a thickness of the order of magnitude 10 nm.

At growth temperatures in the range 220 to 295 ºC, pseudomorph Sn_xSi_{1-x} layers with up to 5 % Sn content have been grown with film thicknesses up to 170 nm. Thermal treatments of these layers at temperatures above 500 ºC for 1 hour led to the formation of α-Sn precipitates, β-Sn precipitates, precipitates that consisted of both α-Sn and β-Sn, and misfit dislocations [5-7]. While these α-Sn precipitates may be considered to constitute QDs in this material system (according to the requirements given above [2]), the simultaneously present misfit dislocations are clearly undesirable for device applications.

Alternatively, temperature and growth rate modulated MBE [8,9] produces Sn_xSi_{1-x}/Si superlattices with essentially pseudomorph Sn_xSi_{1-x} substitutional solutions having Sn compositions in the range of $x = 0.02$ to 0.05 and film thicknesses ranging from 1 to 2 nm. Typical growth procedures [8,9] are as follows.

The growth temperatures of the Sn_xSi_{1-x} layers range from 140 to 170 ºC and the growth rate is 0.02 nm per second. To suppress segregation of Sn to the surface during growth, the Sn_xSi_{1-x} layers are overgrown with 4 to 6 nm of Si at the Sn_xSi_{1-x} growth temperature and at growth rates ranging from 0.01 to 0.03 nm per second. The temperature is then raised to 550 ºC and a Si capping layer with a thickness of the order of magnitude 100 nm is grown at a rate of 0.05 nm per second. By the time this growth sequence has been completed, the Sn_xSi_{1-x} layer has experienced an in situ thermal treatment at 550 ºC for a time of the order of magnitude 30 minutes. For the growth of Sn_xSi_{1-x}/Si multilayer structures, the whole growth sequence is repeated several times, effectively resulting in an

in situ thermal treatment for the first Sn_xSi_{1-x} layer at 550 ºC for a time on the order of magnitude a few hours. In addition to this in situ thermal treatment, ex situ anneals at temperatures between 550 and 900 ºC are performed for 30 minutes. The summarily effect of the epitaxial growth and these thermal treatments is the crystallographically oriented precipitation of Sn within the Si matrix. Precipitation process such as this are broadly described as endotaxy (from the Greek, literally meaning *arrangement within*).

There is an unexplained peculiarity in the plots of average QD precipitate sizes versus ex-situ annealing times, e.g. Fig. 1a, subsequent to temperature and growth rate modulated MBE [9]. Employing analytical transmission electron microscopy in both the parallel illumination and scanning probe mode, we will address this issue in the main part of this paper. A minor issue to be addressed at the end of this paper is the shape of larger (Sn,Si) precipitates.

Thermodynamics driven structural transformations may occur in both α-Sn and Sn_ySi_{1-y} (y > x) QDs. As one can easily estimate, there is an essentially hydrostatic pressure of the order of magnitude 10 GPa on these entities with a corresponding excess Gibbs free energy that significantly exceeds the thermal energy of the atoms in the QDs [10]. This excess Gibbs free energy may be reduced by structural prototype transformations from the diamond structure into either the β-Sn structure or into atomically ordered Sn-Si compounds (over a long enough time, possibly even at room temperature [11]). Here we would like to mention only that we actually did observe in temperature and growth rate modulated MBE grown Sn/Si quantum dot samples β-Sn precipitates [10] and precipitates with showed ½ {110} superlattice spots in their [001] diffraction pattern [12] (besides α-Sn and Sn rich Sn_ySi_{1-y} QD precipitates).

Finally, we would like to remark that the equilibrium shape of a void in Si has been determined experimentally [13] to be a tetrakaidecahedron, Fig. 1b. This shape is determined by {111}, i.e. octahedron, and {100}, i.e. cube, planes. $A = {}^t/_a$ is a shape parameter, Fig. 1b; for A = 0 the shape is an octahedron and $A = {}^2/_3$ corresponds to a cube.

EXPERIMENTAL DETAILS

Three sets of pairs of multilayer samples (one with and one without an additional ex-situ anneal for 30 minutes at 800 ºC) with four Sn_xSi_{1-x}/Si layers and substitutional Sn contents of nominally 2 %, 5 %, and 10 % in each of the Sn_xSi_{1-x} layers were grown by temperature and growth rate modulated MBE [8,9], stored at room temperature for a few years, and eventually selected for our transmission electron microcopy (TEM) investigations.

Our structural analyses employed analytical TEM in both the parallel illumination and scanning probe mode using both a JEOL JEM-2010F Schottky field emission STEM/TEM and a JEOL JEM-3010 TEM at the University of Illinois at Chicago. Parallel illumination TEM utilized conventional diffraction contrast (CTEM), selected area electron diffraction, and high-resolution phase contrast (HRTEM) imaging. Atomic resolution Z-contrast imaging in the scanning probe mode (STEM) proved to be especially useful for our investigations as the effects of strain fields in and around QDs and interference effects such as the formation of moiré fringe due to double diffraction are negligible [12]. In addition, the intensity in Z-contrast images is roughly proportional to the square of the atomic number (Z) of the scattering atoms. For precipitated Sn (Z = 50) in Si (Z = 14), an image contrast as high as about $(50^2/14^2)$ - 1 is possible, which allows for a direct and intuitive interpretation of such Z-contrast images in terms of a distribution map of Sn. TEM specimen preparation followed standard procedures involving mechanical grinding and ion milling to electron transparency.

RESULTS AND DISCUSSIONS

Earlier plan view TEM investigations of Sn_xSi_{1-x} layers annealed at 650 ºC at the California Institute of Technology revealed an initially rapid increase of the average QD volume ($<r>^3$) with time (t) for the first 2.2 hours of the anneal, Fig. 1a, [9]. After this time, the function $<r>^3$(t) showed the typical linear behavior that is expected for precipitate coarsening by volume diffusion [14]. Non-linearities of $<r>^3$ with time are commonly attributed to diffusion shortcuts such as dislocations, stacking faults, grain boundaries, and other common lattice defects [14].

Our TEM/STEM investigations of similar samples in plan view and cross section, Figs. 2a-c, however, showed that these structures are essentially free of the common lattice defects, mentioned above [12]. The lower magnification cross section images of Figs. 2a,b show that there are small precipitates of Sn within the Si matrix quite far away from the spatial positions of the Sn_xSi_{1-x} layers. Such Sn precipitates were found in both the ex-situ annealed and the as grown samples, which only had in situ thermal treatments. Higher magnification Z-contrast STEM images such as Fig. 3a show directly that these Sn precipitates are voids within the Si matrix that are partially filled with Sn. In this (Fig. 3a) image one can directly discern that Sn (which appears brighter due to its larger Z) lines the interface between the void and the Si matrix. As mentioned above, the equilibrium shape of a void in Si is a tetrakaidecahedron, Fig. 1b, [13]. The applications of Neumann's and Curie's symmetry principles [15] to the

determination of the shape of small α-Sn and Sn_ySi_{1-y} precipitates in a Si matrix shows that this can be a tetrakaidecahedron as well [10,16]. Filling an equilibrium shape void in Si by precipitation of Sn should, therefore, be an energetically favorable process.

Additional evidence for the existence of voids in Si that are partly filled with Sn has been gathered by quantitative electron energy loss spectroscopy (EELS) [17], Fig. 3b, and will be presented elsewhere [18]. The filling up of partially Sn filled voids in Si by more Sn as a result of diffusion (into a diffusion shortcut) due to a thermal treatment at moderate parameters (300 °C for approximately three hours) was directly (*in situ*) observed under the electron microscope, Figs. 4a,b. More or less well formed α-Sn QDs, Fig. 4b, resulted as α-Sn and Si both possess the diamond structure. We consider this latter *in situ* observation as most direct proof of our void-filling hypothesis, proposed above.

This mechanism also provides a straightforward explanation for the initially rapid increase of the average QD precipitate volume with annealing time, $<r>^3$ (t), in Fig. 1a. The creation of voids in Si and their subsequent filling with Sn emerges, therefore, as the first of the two mechanisms by which quantum dots grow endotaxially in the Sn/Si system.
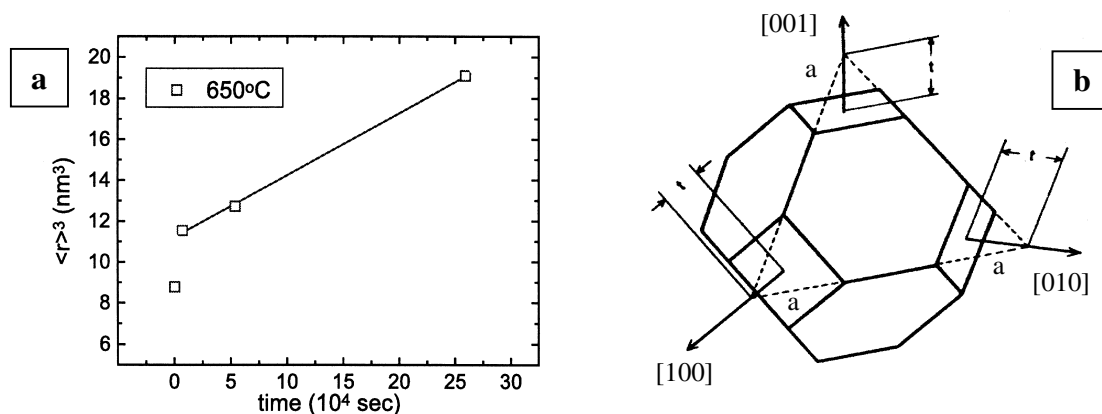

Figure 1. **(a)** Results of earlier ex situ annealing experiments at 650 °C, after ref. [9]. The plot of the average QD precipitate size ($<r>^3$) versus the annealing time (t) shows an initial rapid increase of the $<r>^3$(t) function which later on shows the typical linear relationship that is expected when the precipitate coarsening is governed by volume diffusion. **(b)** Sketch of a tetrakaidecahedron, modified after ref. [15] (with that author's permission).
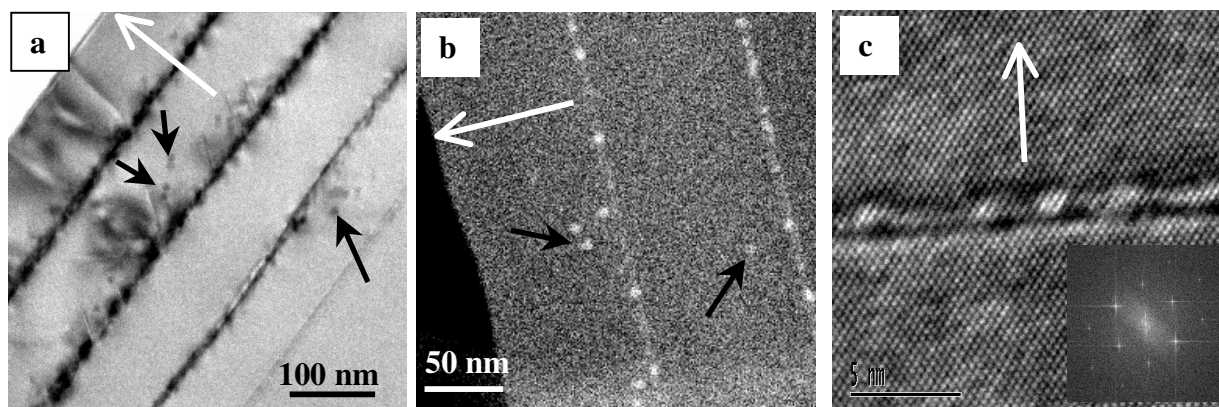

Figure 2. Sn_xSi_{1-x}/Si multilayer structures in [110] cross sections, the smaller black arrows points towards Sn precipitates that grew within the Si layers, the larger white arrows indicate growth directions; **(a)** CTEM overview, x = 0.1, ex-situ annealed; **(b)** Z-contrast STEM overview, x = 0.1, ex-situ annealed; **(c)** HRTEM image showing a perfectly pseudomorph $Sn_{0.02}Si_{0.98}$ layer as deposited, power spectrum as insert.

An interesting question is how these voids may have arisen in the first place. The answer to this question may be found in a mechanism analogously to that described in ref. [19]. According to that mechanism, when a freshly prepared Si surface is exposed to air at room temperature, voids of about 10 nm diameter and a number density of about 10^{10} cm^{-2} form spontaneously approximately 10 nm below the surface due to compressive strain that arises

from the formation of SiO_2 on the surface [19]. Temperature and growth rate modulated MBE deposited Sn_xSi_{1-x} layers may also cause the formation of voids during the (low temperature) growth process since they also compress a freshly grown Si surface. The thermal cycling during temperature and growth rate modulated MBE [8,9] of multilayer structures ensures that there are many vacancies in the structure and this could allow preformed voids of any shape to grow and reach their equilibrium shape.
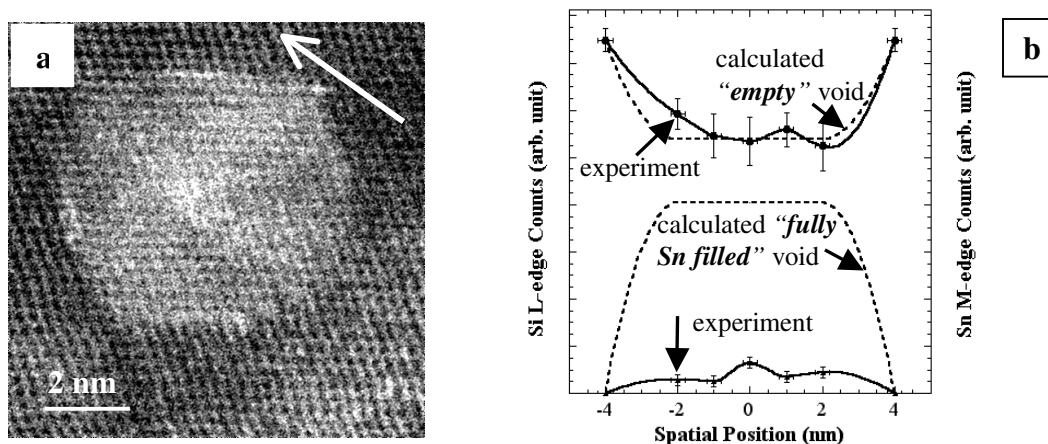
Figure 3. (a) [110] cross section Z-contrast STEM image of a void in Si that is lined by Sn on its interface with the Si matrix. The arrow represents the growth direction, x = 0.1, ex-situ annealed. **(b)** Si L-edge counts and Sn M-edge counts at a series of spatial positions across a void (and along a line perpendicular to the growth direction) in Si that is partly filled with Sn. While the solid circles represent the experimental Si L-edge counts, the triangles represent the experimental Sn M-edge counts. Calculated Si L-edge and Sn M-edge counts are superimposed as dashed lines for both assumptions, that this void is either "empty" or "fully Sn filled". The close proximity of the experimental and calculated sets of Si L-edge counts and the large difference between the respective sets of Sn M-edge counts both indicate that the EELS data are due to a partially Sn filled void in Si. The calculations were performed for a tetrakaidecahedron with A = 0.26 and a specimen thickness of 33 ± 3 nm, as determined experimentally.
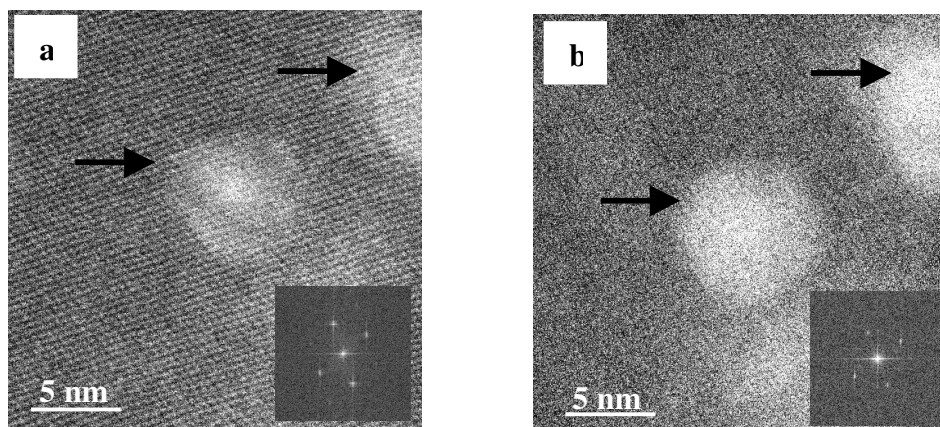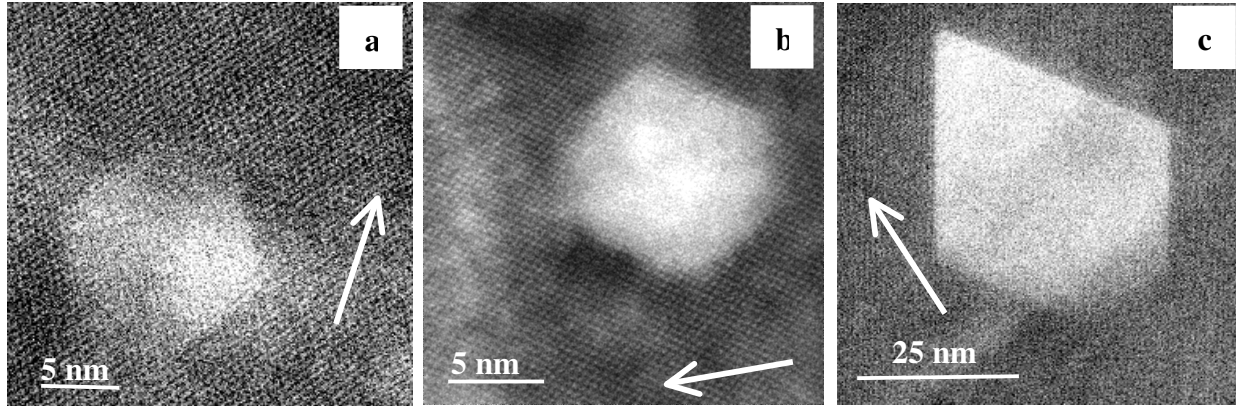

Figure 4. [110] cross section Z-contrast STEM images of α-Sn QD precipitates, x = 0.05, ex-situ annealed, power spectra as inserts; **(a)** Voids in Si that are partially filled with Sn, marked by arrows; **(b)** The same voids but significantly more filled with Sn as a result of a moderate additional thermal treatment (*in situ*) under the STEM.

Phase separation of Sn from a pseudomorph Sn_xSi_{1-x} predecessor layer results in QD precipitates as well since the diamond structural prototype can be conserved. Fig. 5a shows an early stage of the formation of such a QD at the spatial position of a pseudomorph $Sn_{0.1}Si_{0.9}$ layer. When fully formed, these QDs are substitutional solid solutions of Sn in Si (i.e. Sn_ySi_{1-y}) with a higher Sn content than the pseudomorph Sn_xSi_{1-x} predecessor layers (i.e. y > x). We consider this mechanism as the second formation mechanism for endotaxially grown QDs in the Sn/Si system. While we proposed this mechanism earlier on theoretical grounds [9,20], the Z-contrast STEM images, e.g. Fig. 5a, suggest that this phase separation starts with the formation of {111} Sn-Si interfaces and preferential substitutional

Sn-Si replacements in the areas around intersecting {111} planes. Note that only for a very high Sn content, Fig. 5b, is a direct band gap predicted for Sn_xSi_{1-x} alloys [3].

A shape transition with size of Sn rich precipitates that may be due to an increasing contribution of the elastic mismatch strain energy to the total energy of the QDs has been observed, Figs. 5b,c. While smaller α-Sn and Sn rich Sn_ySi_{1-y} QD precipitates possess the typical tetrakaidecahedron shape, Figs. 1b, 4b, and 5b, which probably results from the anisotropy of the interface energy density [16], a much larger precipitate had a shape that resembles more closely an octahedron, Fig. 5c. The shape of this large precipitate may results from the anisotropy of the elastic mismatch strain energy, i.e. the thermodynamics of misfitting precipitates in other words [15].

Figure 5. [110] cross section Z-contrast STEM images, x = 0.1, ex-situ annealed, the arrows represent the respective growth directions; **(a)** Partially formed Sn_ySi_{1-y} precipitate in Si with y > x = 0.1, grown endotaxially by phase separation from a $Sn_{0.1}Si_{0.9}$ layer. Shape transition of Sn rich precipitates with size from **(b)** a tetrakaidecahedron to **(c)** essentially an octahedron.

Intermediately sized Sn rich QD precipitates possess tetrakaidecahedron shapes with smaller {001} facets, i.e. smaller shape parameters suggesting a gradual transition to the shape of an octahedron (A = 0) with increasing size. As the large precipitate in Fig. 5c is located partly at the predecessor substitutional $Sn_{0.1}Si_{0.9}$ solution layer and partly within the Si spacer layer, it may have formed by the simultaneous operation of both endotaxial growth mechanisms. The upper part of the QD may, therefore, consist of α-Sn and the lower part of a substitutional Sn_ySi_{1-y} solution with a high Sn content. This hypothesis is consistent with the contrast in Fig. 5c as there seems to be comparatively less Sn in the center of this precipitate that around its {111}/(001) apex.

Finally, we would like to suggest that the employment of the void creation and subsequent filling mechanism (by with α-Sn precipitate QDs grow endotaxially in Si) may offer an opportunity to make progress in other QD systems such as endotaxially grown (In,As,Si) QDs in Si [21]. With the equilibrium shape of the voids [13] may probably also be connected an equilibrium size so that QDs with a rather homogenous size distribution may be created by the employment of the newly proposed mechanism.

SUMMARY AND CONCLUSIONS

Two distinct mechanisms for the endotaxial growth of quantum dots in the Sn/Si system have been observed. The first of these mechanisms is of a novel type and involves the creation of voids in the Si matrix and their subsequent filling with Sn atoms by diffusion. The second mechanism results from phase separation, as proposed earlier. While the QDs that result from the first mechanism consist of pure α-Sn, the quantum dots that result from the second mechanism are substitutional Sn_ySi_{1-y} solutions with a high Sn content. Both of these mechanisms result in QDs which possess the diamond structure and the typical shape of a tetrakaidecahedron. Sn precipitates that are several times larger than the typical quantum dot possess an essentially octahedral shape.

ACKNOWLEDGMENTS

REFERENCES

[1] D. Bimberg, "Quantum dots: Paradigm changes in semiconductor physics", *Semiconductors* **33,** 951-955 (1999).

[2] N.N. Ledentsov, V.M. Ustinov, V.A. Shchukin, P.S. Kop'ev, Zh.I. Alferov, and D. Bimberg, "Quantum dot heterostructures: fabrication, properties, lasers (Review)", *Semiconductors* **32**, 343-365 (1998).

[3] R.A. Soref and C.H. Perry, "Predicted band gap of the new semiconductor SiGeSn", *J. Appl. Phys.* **69**, 539-541 (1991).

[4] S.Y. Shiryaev, J. Lundsgaard Hansen, P. Kringhøj, and A.N. Larsen, "Pseudomorphic $Si_{1-x}Sn_x$ alloy films grown by molecular beam epitaxy on Si", *Appl. Phys. Lett.* **67**, 2287-2289 (1995).

[5] M.F. Flyn, J. Chevallier, J. Lundsgaard Hansen, and A. Nylandsted Larsen, "Relaxation of strained, epitaxial $Si_{1-x}Sn_x$", *J. Vac. Sci. Technol. B* **16**, 1777-1785 (1998).

[6] M.F. Flyn, J. Chevallier, A.Nylandsted Larsen, R. Feidenhans'l, and M. Seibt, "α-Sn and β-Sn precipitated in annealed $Si_{0.95}Sn_{0.05}$", *Phys. Rev. B* **60**, 5770-5777 (1999).

[7] C. Ridder, M. Fanciulli, A. Nylandsted Larsen, and G. Weyer, "Precipitation of Sn in metastable, pseudomorphic $Si_{0.95}Sn_{0.05}$ films grown by molecular beam epitaxy", *Mater. Sci. Semicond. Processing* **3**, 251-255 (2000).

[8] K.S. Min and H.A. Atwater, "Ultrathin pseudomorphic Sn/Si and Sn_xS_{1-x}/Si heterostructures", *Appl. Phys. Lett.* **72**, 1884-1886 (1998).

[9] R. Ragan, K.S. Min, and H.A. Atwater, "Direct energy gap group IV semiconductor alloys and quantum dot arrays in Sn_xGe_{1-x}/Ge and Sn_xSi_{1-x} /Si alloy systems", *Mater. Sci. Engin. B* **87**, 204-213 (2001).

[10] P. Möck, Y. Lei, T. Topuria, N.D. Browning, R. Ragan, K.S. Min, and H.A. Atwater, "Structural and Morphological Transformations in Self-assembled Sn Quantum Dots in Si Matrix", *Proc. 2003 Nanotechnology Conference and Trade Show*, Vol. **3**, 74-77, 2003.

[11] P. Möck, T. Topuria, N.D. Browning, M. Dobrowolska, S. Lee, J.K. Furdyna, G.R. Booker, N.J. Mason, and R.J. Nicholas, "Internal self-ordering in In(Sb,As), (In,Ga)Sb and (Cd,Mn,Zn)Se nano-agglomerates/quantum dots", *Appl. Phys. Lett.* **79**, 946-948 (2001).

[12] P. Möck, Y. Lei, T. Topuria, N.D. Browning, R. Ragan, K.S. Min, and H.A. Atwater, "Structural transformations in self-assembled semiconductor quantum dots as inferred by transmission electron microscopy", *Physical Chemistry of Interfaces and Nanomaterials*, Jin Z. Zhang, Zhong L. Wang, Eds. Proc. of SPIE Vol. **4807,** 71-82 (2002).

[13] D.J. Eaglesham, A.E. White, L.C. Feldman, N. Moriya, and D.C. Jacobson, "Equilibrium Shape of Si", *Phys. Rev. Lett.* **70**, 1643-1646 (1993).

[14] D.A. Porter and K.E. Easterling, *Phase Transformations in Metals and Alloys*, Chapman & Hall, London, New York, 1992.

[15] W.C. Johnson, "Influence of Elastic Stress on Phase Transformations", in: *Lectures on the Theory of Phase Transformations*, 2nd Edition, Ed. H.I. Aaronson, The Minerals, Metals & Materials Society, Warrendale, 2001.

[16] Neumann's symmetry principle, $\frac{4}{m}\,\bar{3}\,\frac{2}{m} \cap \frac{4}{m}\,\bar{3}\,\frac{2}{m} = \frac{4}{m}\,\bar{3}\,\frac{2}{m}$, yields as the polyhedra that are consistent with the point symmetry group of the interface energy density a tetrakaidecahedron, an octahedron, and a cube. Out of these polyhedra, the tetrakaidecahedron possesses the least symmetry as it has a shape parameter. The shapes of small misfitting precipitates are usually dominated by the anisotropy of the interface energy density [15] and the smallest Sn precipitates should, therefore, possess the shape of a tetrakaidecahedron. Since the lattice mismatch stress (pressure) is essentially hydrostatic, i.e. isotropic, Curie's symmetry principle, $\infty\infty\infty \cap \frac{4}{m}\,\bar{3}\,\frac{2}{m} = \frac{4}{m}\,\bar{3}\,\frac{2}{m}$, yields no influence of the misfit stress field on the anisotropy of the interface energy density.

[17] Y. Lei, "Atomic scale analysis of semiconductor quantum dots by scanning transmission electron microscopy", *PhD thesis*, 2003, University of Illinois at Chicago.

[18] Y. Lei, P. Möck, T. Topuria, N.D. Browning, R. Ragan, K.S. Min, and H.A. Atwater, "Void Mediated Formation of Sn Quantum Dots in a Si Matrix", *Appl. Phys. Lett.,* accepted.

[19] S.H. Lin, I. Mack, N. Pongkrapan, and P. Fraundorf, "Ten-nanometer surface intrusions in room temperature silicon", *Electrochem. & Solid State Lett.* **5**, G83-G85 (2002), con-mat/0110393.

[20] K.S. Min, "Synthesis and Properties of Light-Emitting Si-Based Nanostructures", *PhD thesis*, 1999, California Institute of Technology.

[21] N.D. Zakharov, P. Werner, U. Gösele, R. Heitz, D. Bimberg, N.N. Ledentsov, V.M. Ustinov, B.V. Volovik, Zh. I. Alferov, N.K. Poluakov, V.N. Petrov, V.A. Egorov, and G.E. Cirlin, "Structure and optical properties of Si/InAs/Si layers grown by molecular beam epitaxy on Si substrate", *Appl. Phys. Lett.* **76**, 2677-2679 (2000).